

Chaos synchronization of optoelectronic coupled semiconductor lasers ring

Z.-C. Gao · Z.-M. Wu · L.-P. Cao · G.-Q. Xia

Received: 6 March 2009 / Revised version: 10 July 2009 / Published online: 12 September 2009
© Springer-Verlag 2009

Abstract In this paper, we propose a chaos synchronization configuration based on the optoelectronic coupled semiconductor lasers ring (OCSLR). The synchronization characteristics between semiconductor lasers (SLs) under unidirectional or bidirectional OCSLR are numerically investigated, and the influences of some typical internal and external mismatched parameters on synchronization are simultaneously discussed. The results show that, compared with a unidirectional OCSLR, the bidirectional OCSLR possesses better synchronization properties and robustness to the mismatched parameters. Moreover, the extraction of the encoded signals is preliminarily examined under the chaos shift keying scheme.

PACS 42.55.Px · 42.65.Sf

1 Introduction

Since chaos synchronization was put forward firstly by Pecora et al. in 1990 [1], it has received a great deal of interest due to its potential applications in various research fields.

Z.-C. Gao · Z.-M. Wu · L.-P. Cao · G.-Q. Xia (✉)
School of Physics, Southwest University, Chongqing 400715,
China
e-mail: gqxia@swu.edu.cn
Fax: +86-23-68254609

G.-Q. Xia
Key Laboratory of Weak Light Nonlinear Photonics of Ministry
of Education, Nankai University, Tianjin 300457, China

L.-P. Cao
Elementary Education College, Chongqing Normal University,
Chongqing 400700, China

As one aspect of applications, optical chaos, chaos synchronization and communication based on semiconductor lasers (SLs) subject to external perturbations have been paid special attention in the last two decades [2–28]. Generally, the chaotic carrier can be generated by SL with optical feedback, optoelectronic feedback or optical injection. By synchronizing a receiver laser to a transmitter laser, messages masked in the chaotic carrier can be extracted at the receiver. Extensive research efforts have been concentrated on unidirectional transmission from a transmitter laser to a receiver laser. With the development of relevant investigations and technologies, bidirectional (or multiple directional) transmission [12–16] and chaos synchronization among three or above SLs [17–22] have attracted much attention in recent years. For example, Vicente et al. proposed simultaneous bidirectional message transmission through a partially transparent optical mirror placed in the pathway connecting two SLs [13]. Zhang et al. theoretically investigated a chaos communication system with extremely asymmetrical bidirectional injections [14] and network communication technology using mutually coupled SLs [15]. Chaos synchronization and communication of a chain of semiconductor lasers have been investigated experimentally and theoretically [17–22]. Buldú et al. [12] proposed a novel structure of an optical injection coupled semiconductor lasers ring, and theoretically studied unidirectional and bidirectional chaos synchronization properties among these SLs.

Different systems have different characteristics regarding chaos synchronization. For optical feedback and optical injection systems, the frequency, phase and amplitude of the laser field participate in the dynamics of these systems, and a frequency detuning of even a few hundred MHz between the transmitter and receiver lasers could lead to a large degradation of the synchronization. As for an optoelectronic coupling or feedback system [4, 25, 26], though there always

exists a bandwidth limitation from the components such as the amplifiers and the photodetectors, it has received great interest because it does not require fine frequency matching between the transmitter and receiver lasers. Compared with optical feedback and optical injection, optoelectronic coupling or feedback is flexible and reliable because of its insensitivity to optical phase variations and its convenience to be electrically controlled [25]. In this paper, by drawing lessons from Ref. [12] where optical injection coupling is taken into consideration, we propose a configuration of an optoelectronic coupled semiconductor lasers ring (OCSLR), and unidirectional and bidirectional synchronization characteristics, and the influences of some typical internal and external mismatched parameters on synchronization are investigated.

2 Model

Figure 1 is the schematic of the bidirectional OCSLR configuration, where the inner ring and outer ring respectively represent counterclockwise and clockwise coupling, and the solid lines and dashed lines indicate the electronic paths and the optical paths, respectively. The output light of one laser is converted into an electronic signal by a photodetector (PD), after being amplified by an amplifier (A), and then injects into the next laser. Figure 1 can also be used to the case of unidirectional OCSLR after moving one of the coupled rings.

The rate equations for each laser in the bidirectional OCSLR system can be described as [3, 8, 11]

$$\frac{dS_m}{dt} = -\gamma_{cm} S_m + \Gamma g_m S_m + 2\sqrt{S_0 m S_m} F_{sm}, \quad (1)$$

$$\begin{aligned} \frac{dN_m}{dt} = & \frac{J_m}{ed_m} \left[1 + \kappa_m \frac{S_{fc}(t-\tau)}{S_{0m}} + \sigma_m \frac{S_{fcc}(t-\tau)}{S_{0m}} \right] \\ & - \gamma_{sm} N_m - g_m S_m \end{aligned} \quad (2)$$

where the subscript m indicates the m th ($m = 1, 2, 3$) laser, and the subscripts fc and fcc correspond the lasers near the

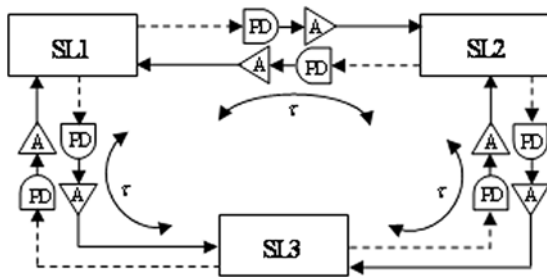


Fig. 1 Schematic of the bidirectional OCSLR configuration, where the solid lines and dashed lines indicate the electronic paths and the optical paths, respectively. SL: semiconductor laser, PD: photodetector, A: amplifier

m th laser in the clockwise and counterclockwise directions, respectively. S is the laser photon density, S_0 is the free-running photon density, N is the carrier density, J is the bias current density, g is the optical gain coefficient, Γ is the confinement factor, γ_c is the cavity photon decay rate, γ_s is the spontaneous carrier decay rate, e is the electronic charge, d is the active layer thickness, κ and σ are the dimensionless coupled parameters in the clockwise and counterclockwise directions, respectively, τ is the coupled time. F_s is the Langevin noise-source term and $\langle F_s(t)F_s(t') \rangle = R_{sp}/2|A_0|^2\delta(t-t')$, where R_{sp} is the rate of spontaneous emission into the laser mode, $A_0 = (\hbar\omega_0 S_0 / 2\epsilon n^2)^{1/2}$ is the steady-state field amplitude of the laser in the free-running condition, \hbar is the Planck constant, ω_0 is the center optical frequency, n is the refractive index of the semiconductor medium, ϵ is the permittivity of free space.

For simplification, numerical calculations are performed on the following normalized dimensionless rate equations:

$$\begin{aligned} \frac{d\tilde{S}_m}{dt} = & \frac{\gamma_{cm}\gamma_{nm}}{\tilde{J}_m\gamma_{sm}} \tilde{N}_m(\tilde{S}_m + 1) - \gamma_{pm}\tilde{S}_m(\tilde{S}_m + 1) \\ & + 2\sqrt{\tilde{S}_m + 1} F_{sm} \end{aligned} \quad (3)$$

$$\begin{aligned} \frac{d\tilde{N}_m}{dt} = & \gamma_{sm}\kappa_m(1 + \tilde{J}_m)[1 + \tilde{S}_{fc}(t-\tau)] \\ & + \gamma_{sm}\sigma_m(1 + \tilde{J}_m)[1 + \tilde{S}_{fcc}(t-\tau)] \\ & - \gamma_{sm}\tilde{J}_m\tilde{S}_m - \gamma_{sm}\tilde{N}_m - \gamma_{nm}\tilde{N}_m(1 + \tilde{S}_m) \\ & + \frac{\gamma_{sm}\gamma_{pm}}{\gamma_{cm}} \tilde{J}_m\tilde{S}_m(1 + \tilde{S}_m) \end{aligned} \quad (4)$$

where the dimensionless variables are defined as $\tilde{S} \equiv (S - S_0)/S_0$, $\tilde{N} \equiv (N - N_0)/N_0$ and $\tilde{J} \equiv (J/ed - \gamma_s N_0)/\gamma_s N_0$ with respect to the free-running values S_0 and N_0 . $\gamma_n = g_n S_0$, where $g_n = \partial g / \partial N$ is the differential gain parameter, and $\gamma_p = -\Gamma g_p S_0$, where $g_p = \partial g / \partial S$ is the nonlinear gain parameter.

3 Results and discussion

The rate equations (3) and (4) can be solved numerically by a fourth-order Runge–Kutta method. During the simulations, the data used are: $R_{sp}/|A_0|^2 = 2.5 \times 10^6 \text{ s}^{-1}$, $\gamma_c = 2.4 \times 10^{11} \text{ s}^{-1}$, $\gamma_s = 1.458 \times 10^9 \text{ s}^{-1}$, $\tilde{J} = 1/3$, $\gamma_n = 3\tilde{J} \times 10^9 \text{ s}^{-1}$, $\gamma_p = 3.6\tilde{J} \times 10^9 \text{ s}^{-1}$, $\tau = 3 \text{ ns}$.

3.1 Chaos synchronization of the SLs in the unidirectional and bidirectional OCSLR

Figure 2 shows the transient output intensity of the three SLs in the unidirectional ($\kappa = 0.1$, $\sigma = 0$) and bidirectional ($\kappa = \sigma = 0.06$) OCSLR, respectively. The output of the

lasers is irregular and of a noise-like sub-nanosecond pulse waveform. As shown in Fig. 2(a), the outputs of these lasers appear to have a time delay in the unidirectional OCSLR,

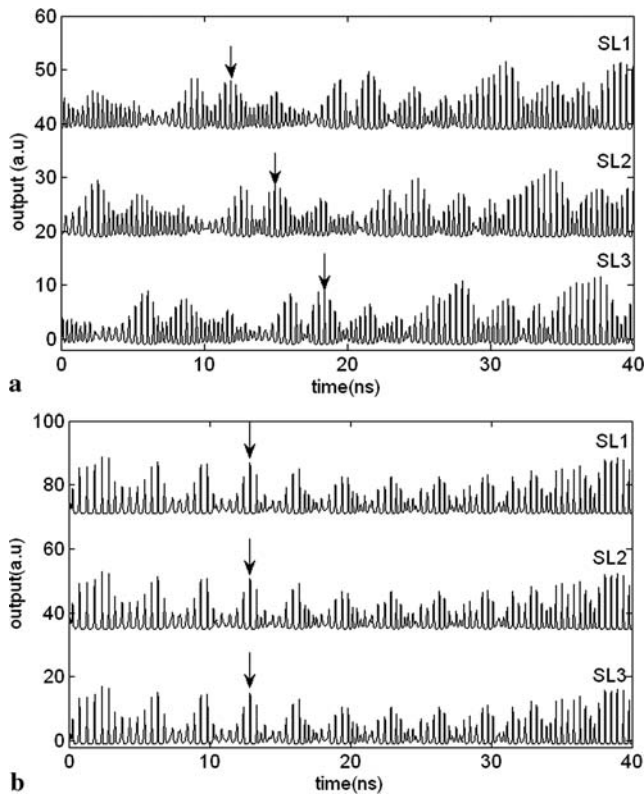


Fig. 2 Transient output intensity of the three lasers in the unidirectional OCSLR (a) and bidirectional OCSLR (b)

while a zero time-lag can be observed in the bidirectional OCSLR.

To evaluate the quality of synchronization between these lasers, one usually uses following cross-correlation function:

$$C_{mn}(\Delta t) = \frac{\langle [S_m(t) - \langle S_m(t) \rangle][S_n(t + \Delta t) - \langle S_n(t) \rangle] \rangle}{\langle |S_m(t) - \langle S_m(t) \rangle|^2 \rangle^{1/2} \langle |S_n(t) - \langle S_n(t) \rangle|^2 \rangle^{1/2}} \quad (5)$$

where S_m and S_n represent the transient output intensity of the m th and n th lasers, respectively, Δt is a time shift between laser outputs, the brackets $\langle \cdot \rangle$ represent the time average. The larger the $|C|$ is, the better synchronization characteristics between the lasers will be. When $C = 1$, the system completely achieves chaos synchronization.

In Fig. 3, we plot the cross-correlation function between each two lasers of the three lasers in the unidirectional and bidirectional OCSLR, respectively. For the case of unidirectional OCSLR, the maximum value of the cross correlation is about 0.83 and located at $\Delta t = 3$ ns, which indicates that the time delay between lasers is equal to the coupling time $\tau = 3$ ns. Additionally, it can also be observed that the role of leader switches randomly from one laser to the other. The above results are similar to that of a unidirectional optical injection coupled semiconductor lasers ring. In the case of the bidirectional OCSLR, the cross correlation has a maximum value higher than 0.99 as shown in Fig. 3(b), which corresponds to a very good level of synchronization. It should be pointed out that the maximum of the cross correlation can

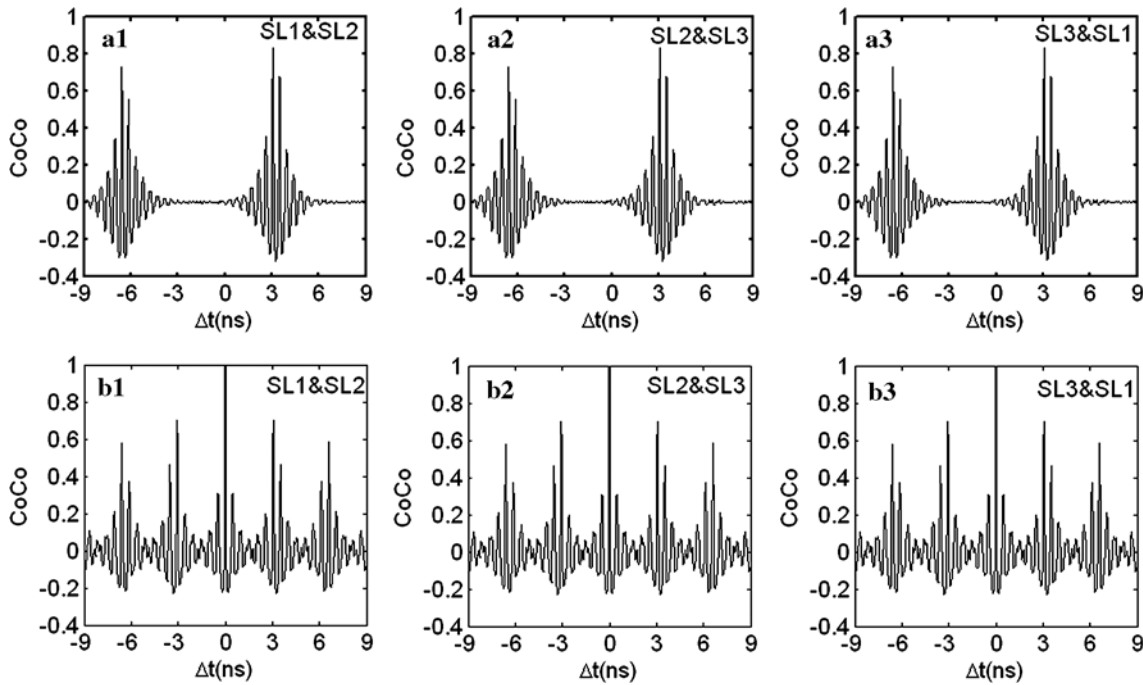


Fig. 3 Cross-correlation functions in the unidirectional OCSLR (a) and bidirectional OCSLR (b)

even reach 1 if the spontaneous emission noise is ignored. In addition, the peak cross correlation located at $\Delta t = 0$ indicates that these SLs have realized zero time-lag synchronizations. So the synchronization characteristics in the bidirectional OCSLR are prior to that of in the unidirectional OCSLR.

3.2 Influence of the mismatched parameters on the chaos synchronization

In order to obtain good chaos synchronization, it is important to match corresponding parameters. However, in practice, perfect parameter matching is difficult to realize. In the following, we will discuss the influences of some typical internal and external mismatched parameters on the quality of chaos synchronization. Here, we consider two internal mismatched parameters, namely γ_c and γ_s , and three external mismatched parameters of \tilde{J} , τ and $\kappa(\sigma)$. For convenience, the mismatched parameters of γ_c , γ_s and \tilde{J} are defined by only changing the relevant parameters of SL2 and fixing the corresponding parameters of SL1 and SL3, while the mismatched parameters of τ and $\kappa(\sigma)$ are defined by only changing the relevant values between SL2 and SL3 and fixing the corresponding values between SL1 and SL2 and between SL3 and SL1 in the clockwise and counterclockwise coupling.

Through calculating the maximum cross-correlation function under these mismatched parameters, one can examine the influences of these mismatched parameters on the quality of the synchronization. The results for unidirectional (left column) and bidirectional OCSLR (right column) are shown in Fig. 4, where the mismatched parameters range from -10% to 10% . From this diagram, it can be seen that in the unidirectional OCSLR, the maximum cross-correlation function between each two lasers almost has the same variation trend with the change of the mismatched parameters. However, in the bidirectional OCSLR, the synchronization variation trend is different. The mismatched γ_c has no influence on the synchronization between SL1 and SL3, and the maximum cross-correlation function has the same change for SL1 and SL2, SL2 and SL3. For mismatched γ_s , perfect chaos synchronization between each two lasers can be obtained, and the maximum cross-correlation function is higher than 0.995. The mismatched \tilde{J} has no influence on the synchronization between SL1 and SL3. However, between SL1 and SL2 and between SL3 and SL2, the synchronization performance with the positive mismatch is better than that with a negative mismatch. Because we only change the \tilde{J} value of SL2 for simplification, it can be anticipated that the mismatched parameter \tilde{J} has an obvious influence on the synchronization of such a bidirectional OCSLR system. For the mismatched $\kappa(\sigma)$, it has a good level of synchronization between all pairs of the SLs with the maximum

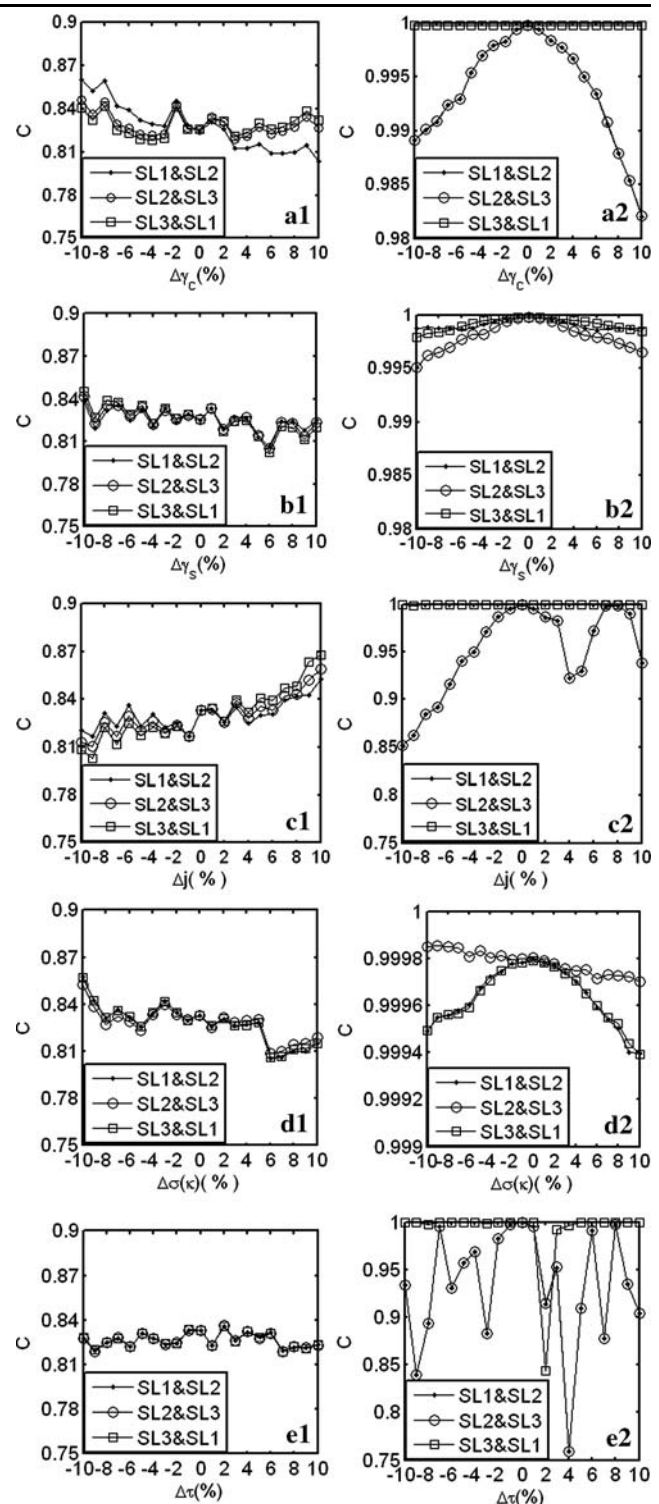
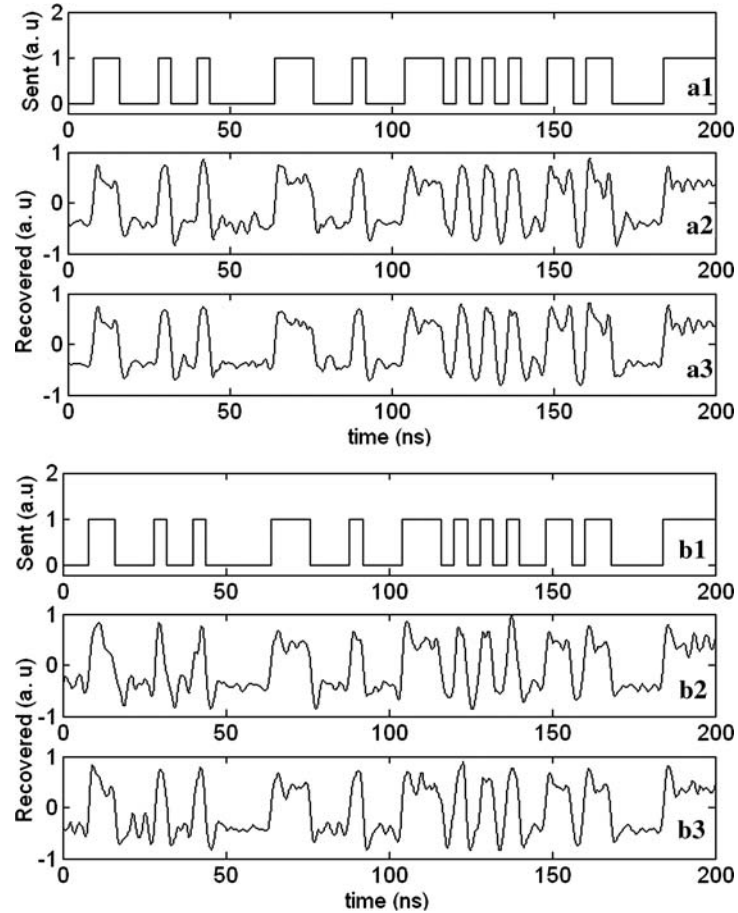


Fig. 4 Maximum of the cross correlation function versus the relative mismatched parameters for unidirectional OCSLR (left column) and bidirectional OCSLR (right column), where (a), (b), (c), (d) and (e) correspond to mismatched γ_c , γ_s , \tilde{J} , $\kappa(\sigma)$ and τ , respectively

cross-correlation function higher than 0.999. But for the mismatched τ , its effect on the synchronization performance

Fig. 5 Waveforms of the encoding and decoding signals, (a) without mismatched parameters, (b) with mismatched parameter, $\Delta\gamma_s = 2\%$



is extensive, and there exist large fluctuations. Calculations show that the dynamics of the SLs may be rendered into the periodical state under some mismatched values. This indicates that the synchronization performance is more sensitive to the coupling time compared with other parameters, and sometimes the variation of the coupling time may change the output dynamics of lasers. Further calculations show that for such bidirectional OCSLR an almost zero time-lag can still be obtained within a given range of mismatched τ . In other words, the bidirectional OCSLR has a better robustness to the mismatched parameters compared with that in the unidirectional OCSLR. By the way, it should be pointed out that the above results are obtained under taking into account only one mismatched parameter. And in practice, there always simultaneously exist multiple mismatched parameters. Under this condition, the system synchronization may further worsen. Therefore, one should select SLs with good parameters matching in order to improve the system synchronization quality.

3.3 Signal transmission in the bidirectional OCSLR

The bidirectional OCSLR has good synchronization properties and robustness to mismatched parameters. We will sim-

ply examine the communication performances in this section. The approach is that a message is encoded at one laser and is recovered at another one. Several encoding and decoding schemes including chaos shift keying (CSK), chaos masking (CMS) and chaos modulation (CM), have been demonstrated for chaotic secure communication. Here, we employ chaos shift keying (CSK) [27]. The binary signal is introduced at SL1 by varying its injection current, and it is recovered at SL2 or SL3 through a fourth-order Butterworth low pass filter with the cutoff frequency at 1.1 times of the signal frequency. During the simulations, the amplitude of message is 1.8% of the pumping current and the signal frequency is 250 MHz.

Figure 5(a1) and (b1) show pseudo-random messages that are introduced into SL1 by current modulation, while Fig. 6 displays the power spectrum of these three SLs under un-modulated (a) and modulated (b) cases. From this diagram, one can observe that the messages can be well hidden into the chaotic carriers. Figure 5(a2) and (a3) give the recovered messages at the SL2 and SL3 parts in the situation without mismatched parameters, respectively, while Fig. 5(b2) and (b3) are the results for $\Delta\gamma_s = 2\%$. From these diagrams, it can be seen that messages can be re-

Fig. 6 Power spectrum of these three SLs in un-modulated (**a**) and modulated (**b**) cases

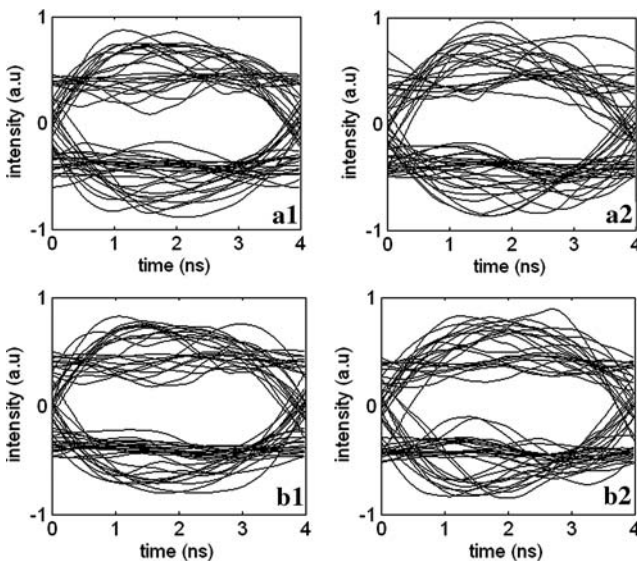
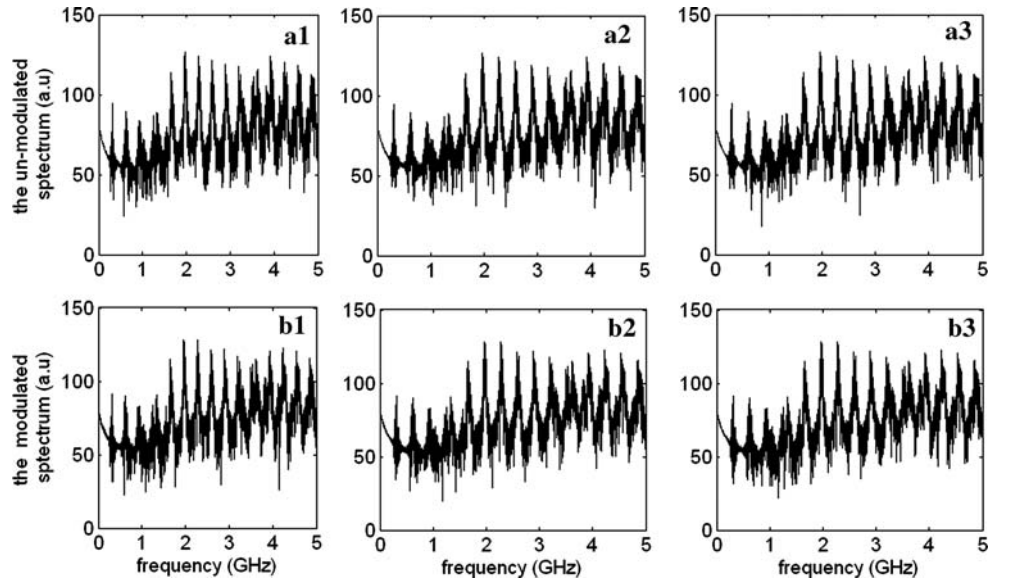


Fig. 7 Eye diagrams of the recovered messages without mismatched parameters (left column) and with mismatched parameter, $\Delta\gamma_s = 2\%$ (right column), where (**a**) and (**b**) denote the eye diagrams of the recovered messages at SL2 and SL3, respectively

covered, and the mismatched parameter γ_s of the lasers has some influence on the decoding message, but the effect is not obvious due to the weak influence of the mismatched parameter γ_s on the system synchronization (see Fig. 4(b2)). Furthermore, to evaluate the decoding quality, Fig. 7 presents corresponding eye diagrams without mismatched parameters (left column) and with mismatched parameter $\Delta\gamma_s = 2\%$ (right column), where (a) and (b) denote the eye diagrams of the recovered messages at SL2 and SL3, respectively. From these diagrams, it can be seen that the eye diagrams are obviously open, though they are not perfect enough. Combing Figs. 5 and 7, such an OC-

SLR system can be used to realize secure communications. As for the security of such system, compared with the unidirectional coupling system, the bidirectional one generally has better robustness to the mismatched parameters. However, this does not represent weakening the security. Previous relevant reports [13, 28] have proven that the security of the bidirectional system can be well guaranteed and the detailed descriptions can be found in these references.

4 Conclusions

In this paper, an OCSLR configuration is proposed, and the synchronization characteristics and the influences of the mismatched parameters on synchronization in the unidirectional and bidirectional OCSLR have been investigated. Compared with the unidirectional OCSLR, the bidirectional OCSLR possesses better synchronization characteristics and more robustness to some typical internal and external mismatched parameters. In addition, the communication performances in the bidirectional OCSLR are also investigated under the CSK scheme. For a 250 MHz message sent from one laser, messages can be extracted satisfactorily from another laser. By the way, this approach can be extended to the case of bidirectional OCSLR including more than three SLs.

Acknowledgements This work was supported by the National Natural Science Foundation of China under Project “Investigation on the bidirectional and long-distance fiber chaos security communication system” and the Open Fund of Key Laboratory of Weak Light Nonlinear Photonics, Ministry of Education, China.

References

1. L.M. Pecora, T.L. Carroll, Phys. Rev. Lett. **64**, 821 (1990)
2. G.Q. Xia, Z.M. Wu, J.G. Wu, Opt. Express **13**, 3445 (2005)
3. H.D.I. Barbanel, M.B. Kennel, L. Illing, J.M. Liu, IEEE J. Quantum Electron. **37**, 1301 (2001)
4. J.M. Liu, H.F. Chen, S. Tang, IEEE J. Quantum Electron. **38**, 1184 (2002)
5. M.W. Lee, K.A. Shore, IEEE Photonics Technol. Lett. **18**, 169 (2006)
6. X.F. Li, W. Pan, B. Luo, D. Ma, IEEE J. Quantum Electron. **42**, 953 (2006)
7. R. Lang, K. Kobayashi, IEEE J. Quantum Electron. **16**, 347 (1980)
8. S. Tang, J.M. Liu, IEEE J. Quantum Electron. **37**, 329 (2001)
9. V. Annovazzi-Lodi, S. Donati, A. Scire, IEEE J. Quantum Electron. **32**, 953 (1996)
10. J. Mulet, C.R. Mirasso, T. Heil, I. Fischer, J. Opt. B, Quantum Semiclass. Opt. **6**, 97 (2004)
11. M.C. Chiang, H.F. Chen, J.M. Liu, IEEE J. Quantum Electron. **41**, 1333 (2005)
12. J.M. Buldú, M.C. Torrent, J. Garcia-Ojalvo, J. Lightwave Technol. **25**, 1549 (2007)
13. R. Vicente, C.R. Mirasso, I. Fischer, Opt. Lett. **32**, 403 (2007)
14. W.L. Zhang, W. Pan, B. Luo, X.H. Zou, M.Y. Wang, Z. Zhou, Opt. Lett. **33**, 237 (2008)
15. W.L. Zhang, W. Pan, B. Luo, X.H. Zou, M.Y. Wang, IEEE Photonics Technol. Lett. **20**, 712 (2008)
16. T. Deng, G.Q. Xia, L.P. Cao, J.G. Chen, X.D. Lin, Z.M. Wu, Opt. Commun. **282**, 2243 (2009)
17. S. Sivaprakasam, K.A. Shore, Opt. Lett. **26**, 253 (2001)
18. G.Q. Xia, Z.M. Wu, J.F. Liao, Opt. Commun. **282**, 1009 (2009)
19. M.W. Lee, J. Paul, C. Masoller, K.A. Shore, J. Opt. Soc. Am. B **23**, 846 (2006)
20. I. Fischer, R. Vicente, J.M. Buldú, M. Peil, C.R. Mirasso, M.C. Torrent, J. Garcia-Ojalvo, Phys. Rev. Lett. **97**, 123902 (2006)
21. O. D'Huys, R. Vicente, T. Erneux, J. Danckaert, I. Fischer, Chaos **18**, 037116 (2008)
22. R. Vicente, I. Fischer, C.R. Mirasso, Phys. Rev. E **78**, 066202 (2008)
23. X.F. Wang, G.Q. Xia, Z.M. Wu, J. Opt. Soc. Am. B **26**, 160 (2009)
24. Q. Yang, Z.M. Wu, J.G. Wu, G.Q. Xia, Opt. Commun. **281**, 5025 (2008)
25. E.M. Shahverdiev, K.A. Shore, Chaos Solitons Fractals **38**, 1298 (2008)
26. R. Vicente, S. Tang, J. Mulet, C.R. Mirasso, J.M. Liu, Phys. Rev. E **73**, 047201 (2006)
27. C.R. Mirasso, J. Mulet, C. Masoller, IEEE Photonics Technol. Lett. **14**, 456 (2002)
28. E. Klein, N. Gross, E. Kopelowitz, M. Rosenbluh, L. Khaykovich, W. Kinzel, I. Kanter, Phys. Rev. E **74**, 046201 (2006)